

Solving Relativistic Three-Body Integral Equations in the Presence of Bound States and Resonances

Taylor Powell

Research Experience for Undergraduates, Old Dominion University

Old Dominion University, VA

Thomas Jefferson National Accelerator Facility

Prepared in partial fulfillment of the requirements of the Department of Energy's Office of Science, National Science Foundation, Old Dominion University, and Thomas Jefferson National Accelerator Facility, under the direction of Dr. Raúl Briceño in the Theory division at Thomas Jefferson National Accelerator Facility.

Participant:

~~Signature~~

Research Advisor:

Signature

Solving Relativistic Three-Body Integral Equations in the Presence of Bound States and Resonances

Taylor R. Powell^{1, 2, *}

¹Thomas Jefferson National Accelerator Facility, 12000 Jefferson Avenue, Newport News, Virginia 23606, USA

²Department of Physics, Old Dominion University, Norfolk, Virginia 23529, USA

(Dated: August 4, 2021)

Three-body interactions play an important role throughout modern-day particle, nuclear, and hadronic physics; many experimentally observed reactions of interest for testing the Standard Model result in final states composed of three particles or more. Due to these issues, a full description of three-body interactions from Quantum Chromodynamics is required. The focus of this project was to extend previous results for a two-body subsystem with a bound state to include resonance channels. We first derived a novel single-variable observable, denoted as an intensity distribution, which is proportional to the probability density of the three-body scattering amplitude. We explored this distribution in the context of established results for a two-body subsystem with a bound state. We then implemented a purely resonant two-body Breit-Wigner scattering amplitude and examined the consequences for the three-body intensity distribution. Finally, we developed a model two-body scattering amplitude with both a resonant and a bound state and examined the three-body scattering intensity distribution for this system. For each of these two-body scattering subsystem models, intensity distributions were computed, resulting in novel graphs of relevant scattering behavior.

I. INTRODUCTION

In this work, recent attempts to obtain three-hadron dynamics from quantum chromodynamics (QCD) using lattice QCD are expanded. In particular, this work approaches determining relativistic three-particle scattering amplitudes for three identical scalar particles using the relativistic field theory (RFT) approach, which sums on-shell projected generalized Feynman diagrams to all orders.

Recent work presented a framework for solving these integral equations for weakly interacting systems (i.e. for weak short-distance three-body interactions and weak coupling between particles in the two-body sub-channels) [1] as well as systems in the presence of two-body bound states (i.e. a three-nucleon system where the deuteron, a shallow bound state between two nucleons, can be formed) [2].

Here we examine two additional cases: a system exhibiting resonant behavior in the two-body sector and a system with a combination of a shallow two-body bound state in addition to the resonant behavior. Solutions to the integral equations are obtained by introducing a discretized mesh in momentum space in order to numerically approximate the integral equations as a system of N linear equations.

In the second case, the presence of the two-body bound state results in a pole singularity inside of the integration range, which can cause numerical instabilities. We adopt a standard regularization technique by introducing a finite $+i\epsilon$ to move the pole off of the real axis, thereby avoiding this pole in the integration region. Solutions to the matrix are then extrapolated to the continuum limit through the parameter N .

II. INTEGRAL EQUATIONS

The unsymmetrized three-body scattering amplitude (as presented in Ref. [3]) can be written as:

$$\mathcal{M}_3^{(u,u)}(\mathbf{p}, \mathbf{k}) = \mathcal{D}^{(u,u)}(\mathbf{p}, \mathbf{k}) + \mathcal{M}_{df,3}^{(u,u)}(\mathbf{p}, \mathbf{k}) \quad (1)$$

Where the first term, \mathcal{D} , represents the sum over all possible pair-wise interactions between the bodies mediated by one-particle exchanges. Here, \mathbf{k} and \mathbf{p} are the momenta of one of the hadrons in the initial and final states, respectively. We refer to this hadron as the *spectator*, and the other two particles are called a *pair*. The superscript, (u, u) , indicates the scattering amplitude is unsymmetrized; the fully symmetrized amplitude is obtained by summing

*e-mail: tpowe002@odu.edu

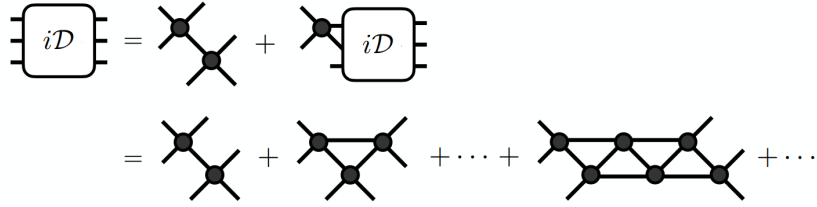


FIG. 1: Diagrammatic representation of the $\mathcal{D}^{(u,u)}$ amplitude defined in Eqn. (3). Black circles represent the on-shell two-particle scattering amplitude \mathcal{M}_2

over all nine possible combinations of spectator momenta. In addition to the momenta of the particles, the amplitude additionally depends on the square of the center-of-mass energy, represented by the Mandelstam variable: $s = E^2$, which is suppressed in the argument list of Eqn. (1). The second term, $\mathcal{M}_{df,3}^{(u,u)}$ represents short-distance three-particle interactions, which we hereafter assume the scattering amplitude is dominated by two-body subprocesses and take the limit as this term approaches zero. Given this assumption, the three-body amplitude is reduced to the ladder portion as,

$$\lim_{\mathcal{M}_{df,3} \rightarrow 0} \mathcal{M}_3^{(u,u)}(\mathbf{p}, \mathbf{k}) = \mathcal{D}^{(u,u)}(\mathbf{p}, \mathbf{k}) \quad (2)$$

The expression for the ladder equation which sums over all pair-wise interactions is defined by the integral equation,

$$\mathcal{D}^{(u,u)}(\mathbf{p}, \mathbf{k}) = -\mathcal{M}_2(p)G(\mathbf{p}, \mathbf{k})\mathcal{M}_2(k) - \mathcal{M}_2(p) \int \frac{d^3\mathbf{k}'}{(2\pi)^3 2\omega_{k'}} G(\mathbf{p}, \mathbf{k}')\mathcal{D}^{(u,u)}(\mathbf{k}', \mathbf{k}) \quad (3)$$

Where \mathcal{M}_2 is the two-body scattering amplitude describing interactions between particles in the pair. The energy of the interacting pair is fixed by the momentum of the spectator, $\sigma_k \equiv (E - \omega_k)^2 - k^2$, where $\omega_k \equiv \sqrt{m^2 + k^2}$ and $k \equiv |\mathbf{k}|$. This ladder amplitude is dependent also on the exchange propagator, G , which describes the long-range interactions between the interacting pair and the spectator and is defined by,

$$G(\mathbf{p}, \mathbf{k}) \equiv \frac{H(p, k)}{b_{pk}^2 - m^2 + i\epsilon} \quad (4)$$

Where $b_{pk}^2 \equiv (E - \omega_p - \omega_k)^2 - (\mathbf{p} + \mathbf{k})^2$ and $H(p, k)$ is a cutoff function defined in Ref. [4] as,

$$H(p, k) \equiv J(\sigma_p/4m^2)J(\sigma_k/4m^2) \quad (5)$$

$$J(x) \equiv \begin{cases} 0, & x \leq 0 \\ \exp\left(-\frac{1}{x} \exp\left[-\frac{1}{1-x}\right]\right), & 0 < x \leq 1 \\ 1, & x > 1 \end{cases} \quad (6)$$

In order to reduce the strength of pole singularities arising from two-particle scattering amplitudes with bound states, we define an amputated amplitude, d , defined by,

$$\mathcal{D}^{(u,u)}(\mathbf{p}, \mathbf{k}) \equiv \mathcal{M}_2(p)d^{(u,u)}(\mathbf{p}, \mathbf{k})\mathcal{M}_2(k) \quad (7)$$

Inserting Eqn. (7) into Eqn. (3), we obtain,

$$d^{(u,u)}(\mathbf{p}, \mathbf{k}) = -G(\mathbf{p}, \mathbf{k}) - \int \frac{d^3\mathbf{k}'}{(2\pi)^3 2\omega_{k'}} G(\mathbf{p}, \mathbf{k}')\mathcal{M}_2(k')d^{(u,u)}(\mathbf{k}', \mathbf{k}) \quad (8)$$

This equation for d is computationally intensive due to the three-dimensional integral over momenta. Using partial wave projection over the total angular momentum, J , and limiting ourselves to the $J = 0$ (or S -wave) component we can integrate over the solid angle to remove the angular dependence of our integral as,

$$d_S^{(u,u)}(p, k) = -G_S(p, k) - \int_0^\infty \frac{dk' k'^2}{(2\pi)^2 \omega_{k'}} G_S(p, k') \mathcal{M}(k') d_S^{(u,u)}(k', k) \quad (9)$$

Where the angular integral for G_S gives,

$$\begin{aligned} G_S(p, k) &\equiv \int \frac{d\Omega_p}{4\pi} \frac{d\Omega_k}{4\pi} G(\mathbf{p}, \mathbf{k}) \\ &= -\frac{H(p, k)}{4pk} \log \left(\frac{\alpha(p, k) - 2pk + i\epsilon}{\alpha(p, k) + 2pk + i\epsilon} \right) \end{aligned} \quad (10)$$

Where $\alpha(p, k) = (E - \omega_k - \omega_p)^2 - p^2 - k^2 - m^2$. In order to conduct a single-variable study of the three-body scattering amplitude both below and above the three-body energetic threshold at $s = (3m)^2$, we derive an observable, denoted as an intensity distribution, which is proportional to the probability density of the three-body scattering amplitude. The details of this derivation are left to Appendix C, but the form of the observable is given by,

$$\begin{aligned} I(s) &= \left| \rho_{\varphi b}(s) \mathcal{M}_{\varphi b}(s) \right|^2 + 2 \int_{4m^2}^{(\sqrt{s}-m)^2} \frac{d\sigma_k}{\pi} \rho(\sigma_k) \tau(s, \sigma_k) \rho_{\varphi b}(s) \left| \mathcal{M}_{\varphi b \rightarrow 3\varphi}(\sigma_k, s) \right|^2 \\ &+ \int_{4m^2}^{(\sqrt{s}-m)^2} \frac{d\sigma_k}{\pi} \int_{4m^2}^{(\sqrt{s}-m)^2} \frac{d\sigma_p}{\pi} \rho(\sigma_p) \rho(\sigma_k) \tau(\sigma_p, s) \tau(\sigma_k, s) \left| \mathcal{M}_3(\sigma_p, s, \sigma_k) \right|^2 \end{aligned} \quad (11)$$

Where $\tau(\sigma_b, s) = \rho_{\varphi b}(s)$, $\mathcal{M}_{\varphi b}(s) = g^2 d_S(\sigma_b, \sigma_b)$, and $\mathcal{M}_{\varphi b \rightarrow 3\varphi}(\sigma_k, s) = g \mathcal{M}_2(\sigma_k) d_S(\sigma_b, \sigma_k)$. This expression can be given more compactly as $I(s) = I_{\varphi b}(s) + 2I_{\varphi b \rightarrow 3\varphi}(s) + I_{3\varphi}(s)$. For any \mathcal{M}_2 containing no bound states, the observable reduces to $I(s) = I_{3\varphi}(s)$.

III. TWO-BODY SCATTERING AMPLITUDES

We consider three separate toy-models of potential 2-body scattering amplitudes: a narrow bound state, a resonance channel, and a combined bound state with resonance. We examine each case in turn.

A. Bound State

Previous work (see Ref. [2]) introduced a toy model for a two-body scattering amplitude containing a single bound state given as,

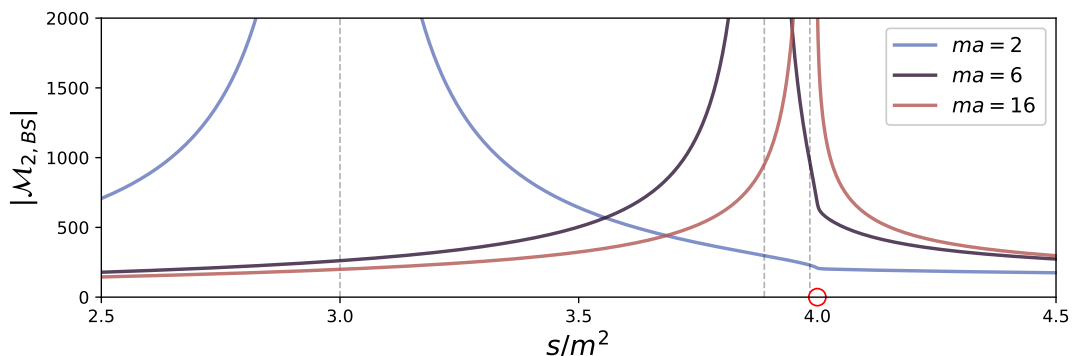


FIG. 2: Plot of $\mathcal{M}_{2,BS}$ with as a function of s/m^2 for scattering lengths $a = \{2, 6, 16\}$. The vertical dashed lines indicate the locations of the bound state poles, and the red circle indicates the threshold.

$$\begin{aligned}\mathcal{M}_{2,BS}(k) &= \mathcal{M}_{2,BS}(\sigma_k) \\ &= \frac{16\pi\sqrt{\sigma_k}}{-1/a - iq_{2k}^*(\sigma_k)}\end{aligned}\quad (12)$$

Where $q_{2k}^*(\sigma_k) = \sqrt{\sigma_k/4 - m^2}$ is the relative momentum between the two particles in their center of mass (CM) frame and the scattering length is a . We can see from Figure 3 this amplitude has a pole on the real σ_k axis, which we label as σ_b , at,

$$\sigma_b = 4(m^2 - 1/a^2) \quad (13)$$

Near the bound state pole, the two-body scattering amplitude has the form,

$$\lim_{\sigma_k \rightarrow \sigma_b} \mathcal{M}_{2,BS}(\sigma_k) = \frac{-g^2}{\sigma_k - \sigma_b} \quad (14)$$

Where g is the residue at the pole. Equating Eqn. (12) to Eqn. (14), we can solve analytically for g :

$$g = 8\sqrt{\frac{2\pi\sqrt{\sigma_b}}{a}} \quad (15)$$

More details on this calculation are found in Appendix A.

B. Resonance Channel

A well-known toy model for a two-body scattering amplitude with a resonance is given by the relativistic Breit-Wigner parameterization,

$$\mathcal{M}_{2,RS}(\sigma_k) = \frac{16\pi\sqrt{\sigma_k}}{q_{2k}^*(\sigma_k) \cot \delta - iq_{2k}^*(\sigma_k)} \quad (16)$$

Where,

$$\tan \delta(s) = \frac{\sqrt{\sigma_k}\Gamma(s)}{m_0^2 - \sigma_k} \quad \Gamma(s) = \frac{g^2 m_0^2}{6\pi \sigma_k} q_{2k}^*(\sigma_k)$$

For this work, we choose the parameter $m_0 = 2.5$ and allowed values for $g = \{2, 3, 4\}$, which affects the width of the resonance channel. Due to the lack of a bound state in this two-particle subsystem, there is no fixed on-shell value for the spectator's momentum. Therefore we choose the spectator's momentum such that it lies in the physical region (above threshold), fix the particle's energy, and scan in the two-particle subsystem's total momentum.

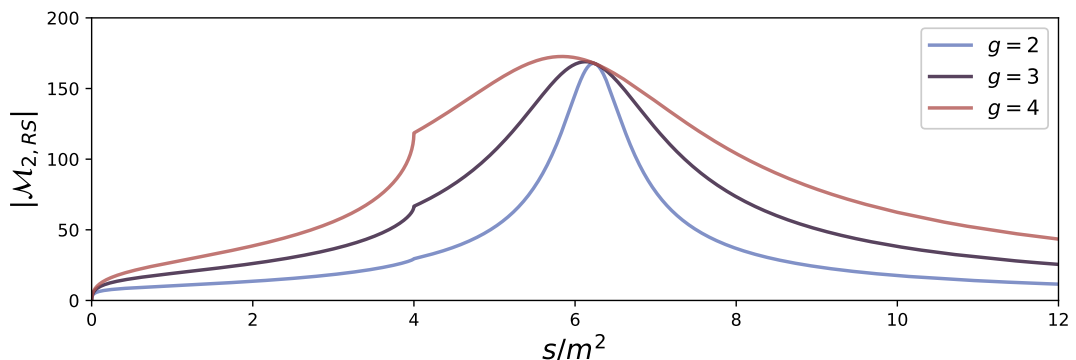


FIG. 3: Plot of $\mathcal{M}_{2,RS}$ (A Breit-Wigner scattering amplitude with a resonance channel) as a function of s/m^2 for $g = \{2, 3, 4\}$.

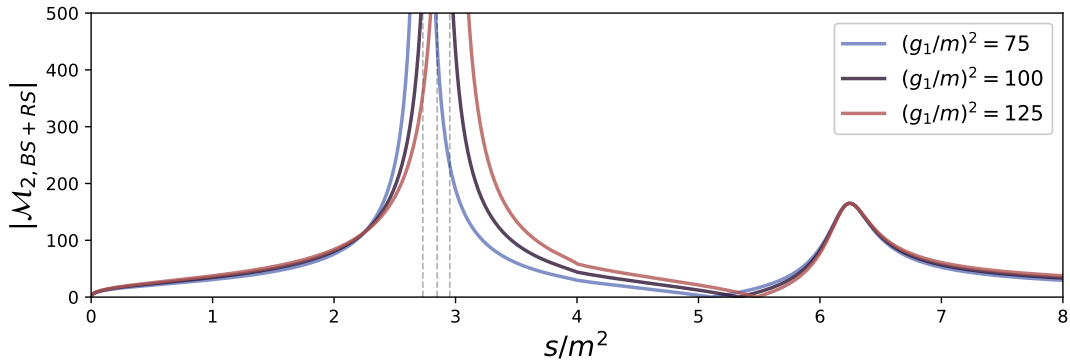


FIG. 4: Plot of $\mathcal{M}_{2,BS+RS}$, a toy-model two-particle scattering amplitude with both a shallow bound state and a resonance channel, as a function of s/m^2 for $(g_1/m)^2 = \{75, 100, 125\}$. The dashed lines indicate the locations of the bound state poles.

C. Combination of Bound State and Resonance Channel

We now consider a generalized form for the two-particle scattering amplitude which exhibits both a bound state and resonance behavior,

$$\mathcal{M}_{2,RS+BS}(\sigma_k) = \frac{\mathcal{K}_2(\sigma_k)}{1 - i\rho(\sigma_k)\mathcal{K}_2(\sigma_k)} \quad (17)$$

Where the 2-body K-matrix has the form,

$$\mathcal{K}_2(\sigma_k) = \frac{g_1^2}{m_1^2 - \sigma_k} + \frac{g_2^2}{m_2^2 - \sigma_k} \quad (18)$$

And we choose the parameters such that $m_1 = 1.5m$, $m_2 = 2.5m$, $g_2^2 = 30m^2$, and allow $g_1^2 = \{75m^2, 100m^2, 125m^2\}$. This results in an amplitude exhibiting the behavior shown in Figure 4. We can then numerically solve for the location of the bound state by choosing σ_b such that $(1 - i\rho(\sigma_b)\mathcal{K}_2(\sigma_b) = 0)$, which results in the poles as seen in Figure 4. Near the bound state, the pole on the real axis again takes the form,

$$\lim_{\sigma_k \rightarrow \sigma_b} \mathcal{M}_{2,RS+BS}(\sigma_k) = \frac{-g^2}{\sigma_k - \sigma_b} \quad (19)$$

Where g is the residue at the pole. Solving analytically for g , we find,

$$g^2 = -16\pi\sqrt{\sigma_b} \frac{\sigma_b\sqrt{4m^2 - \sigma_b}}{g_1^2(m_2^2 - \sigma_b) + g_2^2(m_1^2 - \sigma_b)} \left\{ g_1^2(m_2^2 - \sigma_b) \left(\frac{\sigma_b(4m^2 - \sigma_b)}{2(m_1^2 - \sigma_b)} - m^2 \right) + g_2^2(m_1^2 - \sigma_b) \left(\frac{\sigma_b(4m^2 - \sigma_b)}{2(m_2^2 - \sigma_b)} - m^2 \right) \right\}^{-1} \quad (20)$$

Where the numerical details are found in Appendix B. Of particular note for this two-body amplitude, the modification of the value for $(g_1/m)^2$ has the primary effect of moving the depth of the bound state and slightly widening the pole singularity.

IV. DETAILS OF NUMERICAL METHODS

In order to solve the integral equation presented in Eqn. (9), it is necessary to discretize in terms of the spectator momenta, which we denote with an indexed form as $k' \rightarrow k'_n$ and generate a uniform mesh of values. The minimum value for the spectator's momentum is $k_{\min} = 0$. The maximum value for the momentum is governed by the cutoff

function, $H(p, k)$. The value goes to zero when $\sigma_k = 0$, which then implies $k_{\max}^2 = (s - m^2)^2 / 4s$. The distance between mesh points is given by the transformation of the differential momentum in the integrand as: $dk' \rightarrow \Delta k' = k'_{\max}(s) / N$. We then discretize Eqn. (9) in momenta by,

$$d_S^{(u,u)}(p, k; \epsilon, N) = -G_S(p, k; \epsilon) - \sum_{n=0}^{N-1} \frac{\Delta k' k_n'^2}{(2\pi)^2 \omega_{k_n'}} G_S(p, k_n'; \epsilon) \mathcal{M}_2(k_n'; \epsilon) d_S^{(u,u)}(k_n', k; \epsilon, N) \quad (21)$$

Where the ϵ -dependence of \mathcal{M}_2 is implemented as $\mathcal{M}(\sigma_k; \epsilon) \equiv \mathcal{M}(\sigma_k + i\epsilon)$. We can then solve this equation for d by writing it as a matrix in the space defined by $\{k_n'\}$ with matrix elements given by,

$$d_{S;nn'}^{(u,u)} = d_S^{(u,u)}(k_n, k_{n'}; \epsilon, N) \quad (22)$$

Moving the summation term to the other side,

$$-G_S(p, k; \epsilon) = \sum_{n=0}^{N-1} \left[d_{S;nn'}^{(u,u)}(k_{n'}, k_n; \epsilon, N) \delta_{k_{n'}, k_n} + \frac{\Delta k' k_n'^2}{(2\pi)^2 \omega_{k_n'}} G_S(k_{n'}, k_n; \epsilon) \mathcal{M}_2(k_{n'}; \epsilon) d_{S;nn'}^{(u,u)}(k_{n'}, k_n; \epsilon, N) \right] \quad (23)$$

Where $\delta_{k_{n'}, k_n}$ is the Kronecker delta. We can then define a simple linear system to solve for d at arbitrary (p, k) as,

$$d_S^{(u,u)}(p, k; \epsilon, N) = -[B^{-1} G_S]_{nn'} \Big|_{k_n=p; k_{n'}=k} \quad (24)$$

Where B is a matrix whose elements are defined by,

$$B_{nn'} = \delta_{k_{n'}, k_n} + \frac{\Delta k' k_n'^2}{(2\pi)^2 \omega_{k_n'}} G_S(k_{n'}, k_n; \epsilon) \mathcal{M}_2(k_{n'}; \epsilon) \quad (25)$$

For calculation of the intensity observable contribution from $3\varphi \rightarrow 3\varphi$, $I_{3\varphi}(s)$, d is averaged over all physical (\mathbf{k}, \mathbf{p}) combinations. In the presence of a bound state, the spectator has an on-shell momentum which corresponds to the bound state pole, which we label as q . We can obtain this value by fixing the energy of the two-particle subsystem at the bound state pole, the sum of the energies of the two-body subsystem and the spectator particle satisfy the relation $\sqrt{s} = \sqrt{\sigma_b + q^2} + \sqrt{m^2 + q^2}$. Solving for q gives:

$$q = \frac{1}{2\sqrt{s}} \lambda^{1/2}(s, \sigma_b, m^2) \quad (26)$$

Where $\lambda(x, y, z) = x^2 + y^2 + z^2 - 2(xy + xz + yz)$ is the Källén triangle function. For the $I_{\varphi b}(s)$ term, we interpolate through the matrix to obtain this on-shell value. For the $I_{\varphi b \rightarrow 3\varphi}(s)$ term, we choose $(k = q)$ and interpolate the matrix into a vector form over $p \in \{k_{n'}\}$, which is summed over to find $I_{\varphi b \rightarrow 3\varphi}(s)$. Finally, we directly adopt the error measurement from Ref. [2] such that $\eta \equiv 2\pi N \epsilon_q / k_{\max}$, where ϵ_q is given by,

$$\epsilon_q = \epsilon \left(\frac{s + m^2 - s_b}{4qs} \right) \quad (27)$$

For the two-body scattering amplitude without bound state pole, we may drop the ϵ -dependence for the two-body scattering amplitude, as there is no pole in the integration region for $\mathcal{M}_{2,RS}$. We do, however, still require a well-defined ϵ due to the definition for G_S given in Eqn. (10). In the resonance only case, we define q by fixing the energy of the two-particle subsystem to the two-particle threshold ($\sigma_k \text{ fixed} = (2m)^2 \rightarrow q_{RS} = \lambda^{1/2}(s, \sigma_k \text{ fixed}, m^2) / 2\sqrt{s}$).

V. RESULTS

For each of the two-body scattering amplitudes of interest, we calculate the intensity distribution over an appropriate energetic range.

A. Bound State

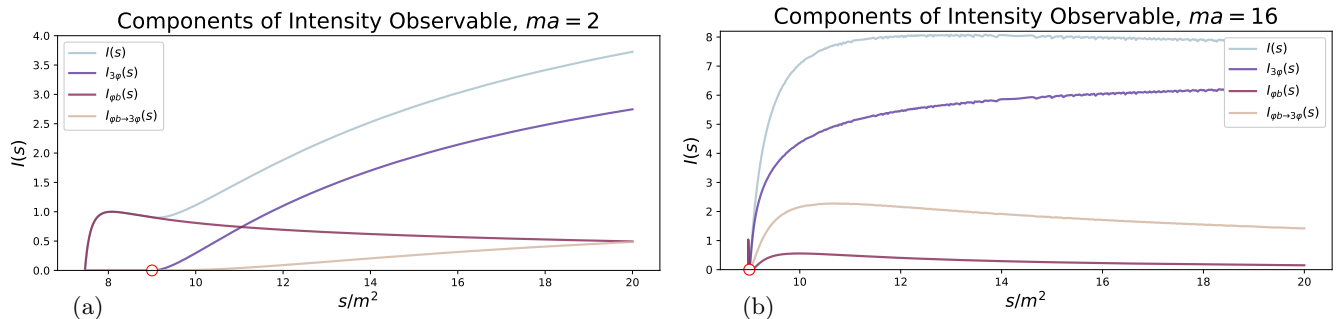


FIG. 5: Plots of $I(s)$ with two-particle scattering amplitude $\mathcal{M}_{2,BS}$ as a function of s/m^2 for scattering lengths (a) $ma = 2$ and (b) $ma = 16$. Each case is broken out by individual component contributions to the total intensity distribution. The red circles indicate the location of the three-body energetic threshold.

In the presence of a two-body bound state, we computed intensity distributions for each of the scattering lengths of interest. The full results are presented in Appendix D, however we present two particular cases in Figure 5 and plot over the energy range $\sigma_b < s < 20m^2$ with the overall intensity distribution broken out by component.

As expected, we see only a $I_{\varphi b}$ contribution below the three-particle energetic threshold at $s = (3m)^2$. Below this threshold, there is insufficient energy in the system for three particles to exist independently, therefore the only physical process allowable requires two of the particles to form a bound state.

For the deeply bound state ($ma = 2$), above threshold, the $I_{\varphi b}$ contribution is non-negligible and monotonically decreasing. We then also see smoothly increasing contributions from the three-particle component, $I_{3\varphi}$, and the exchange component, $I_{\varphi b \rightarrow 3\varphi}$. In contrast, the shallow bound state ($ma = 16$) has a much smaller binding energy, and thus less phase space available for the bound state to exist above the three-particle threshold. Therefore, the contributions from the three-particle and exchange components of the intensity distribution dominate above this threshold.

B. Resonance Channel

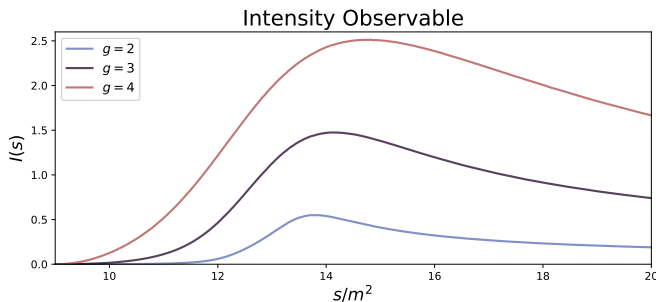


FIG. 6: Plots of $I(s)$ with two-particle scattering amplitude $\mathcal{M}_{2,RS}$ as a function of s/m^2 for select choices of g .

In the case of the resonance channel alone, the intensity distribution is relatively unremarkable, as shown in Figure 6. There is no bound state in the two-body sector, therefore there is only a single contributor to the intensity, $I_{3\varphi}$. We

see a resonance peak in the vicinity of $13 < s/m^2 < 15$. Increasing the width of the two-body resonance channel by increasing the value of g has a corresponding effect of increasing the intensity distribution, as expected.

C. Combined Bound State and Resonance Channel

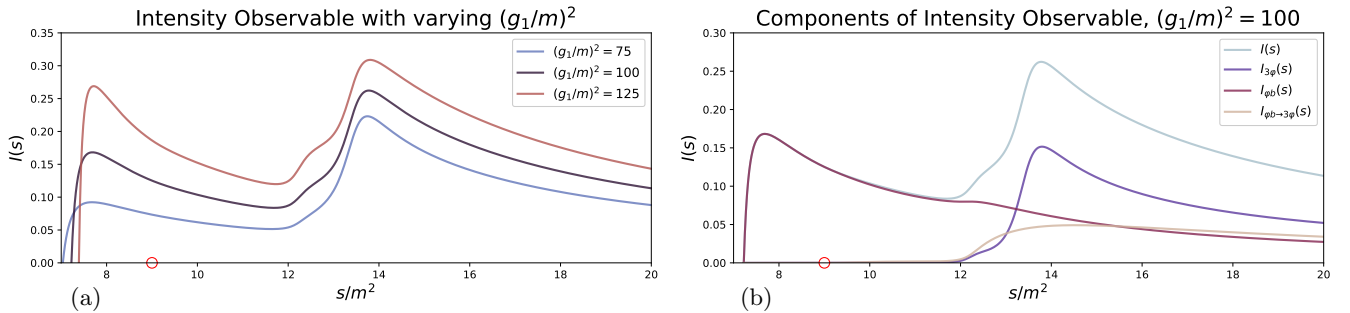


FIG. 7: Plots of $I(s)$ with two-particle scattering amplitude $\mathcal{M}_{2,RS+BS}$ as a function of s/m^2 for (a) varying $(g_1/m)^2$ and (b) broken out by individual component contributions to the total intensity distribution. The red circles indicate the location of the three-body energetic threshold.

In the case of the combined bound state and resonance channel in the two-body sector, the intensity distribution for selected values of $(g_1/m)^2 = \{75, 100, 125\}$ is shown in the left panel of Figure 7. In the right panel of this figure, the individual component contributions to the total are shown for the particular case of $(g_1/m)^2 = 100$.

As discussed when the two-body amplitude was introduced in Section III, the modification of the parameter $(g_1/m)^2$ has the primary effect of moving the location and width of the pole singularity corresponding to the bound state in the two-body sector. In the left panel of Figure 7, increasing the shallowness of the bound state creates a larger peak on the left side of the graph and slightly increases the total intensity of the distribution. Additionally, as $(g_1/m)^2$ increases in this range, we see a more pronounced "bump" in the distribution in the range $12 < s/m^2 < 13$.

In the right panel of Figure 7, the individual contributors to the overall intensity distribution are shown. Going from left to right, there is a peak in the region below the three-body threshold which is driven by the $I_{\varphi b}$ component, since this is the only physical process occurring in this region. There is a "bump" in the distribution in the range $12 < s/m^2 < 13$ (as previously mentioned) which is driven by underlying exchange processes in the $I_{\varphi b \rightarrow 3\varphi}$ component. Finally, there is a pronounced peak near $s/m^2 = 14$ which is driven by the resonance channel in the two-body sector, as similarly seen in the resonance only case.

VI. CONCLUSIONS

In this work, a method for solving relativistic three-body integral equations is adapted from Ref. [2] which allows for numerical solutions for the three-particle scattering amplitude in an exchange-dominated scattering process. We derive a suitable single-variable observable, $I(s)$, which averages over the physical momenta for underlying two-body scattering amplitudes with or without a bound state and is proportional to the three-particle scattering amplitude probability density. This observable is examined in the context of three toy-model two-body scattering amplitudes: bound state only, resonance channel only, and a combination of the two. In the combined case, we see a bump in the overall intensity distribution which is not due to a bound state or resonance channel, but rather, an exchange process in the two-body sector where a bound state is formed or broken during the scattering event.

VII. ACKNOWLEDGEMENTS

I would like to acknowledge Dr. Raúl Briceño and Dr. Andrew Jackura for their continuous support and wisdom through this project. I also thank the Thomas Jefferson National Accelerator Facility, Old Dominion University, and the Science Education team at Jefferson Lab for their support. Finally, I also thank my wife, Brittany, and both of our children for their never-ending patience and support. This work was supported by the REU program through Old Dominion University NSF Grant #1950141.

Appendix A: Calculation of Pole Residue in Bound State Case

Recall the model for the bound state only two-body scattering amplitude given by,

$$\mathcal{M}_{2,BS}(k) = \frac{16\pi\sqrt{\sigma_k}}{-1/a - iq_{2k}^*(\sigma_k)} \quad (\text{A1})$$

Near the bound state pole, the two-body scattering amplitude has the form,

$$\lim_{\sigma_k \rightarrow \sigma_b} \mathcal{M}_{2,BS}(\sigma_k) = \frac{-g^2}{\sigma_k - \sigma_b} \quad (\text{A2})$$

Where g is the residue at the pole. Equating Eqn. (A1) to Eqn. (A2), we can solve analytically for g :

$$-g^2 = \lim_{\sigma_k \rightarrow \sigma_b} (\sigma_k - \sigma_b) \frac{16\pi\sqrt{\sigma_k}}{-1/a - iq_{2k}^*(\sigma_k)} = \lim_{\sigma_k \rightarrow \sigma_b} (\sigma_k - \sigma_b) \frac{-16\pi a \sqrt{\sigma_k}}{1 + iaq_{2k}^*(\sigma_k)} \quad (\text{A3})$$

Expanding the denominator as a Taylor series at $\sigma_k = \sigma_b$,

$$\begin{aligned} 1 + iaq_{2k}^*(\sigma_k) &= \overbrace{(1 + iaq_{2k}^*(\sigma_b))}^0 + (\sigma_k - \sigma_b) \frac{\partial}{\partial \sigma_k} (1 + iaq_{2k}^*(\sigma_b)) \Big|_{\sigma_k = \sigma_b} \\ &\quad + (\sigma_k - \sigma_b) \frac{\partial^2}{\partial \sigma_k^2} (1 + iaq_{2k}^*(\sigma_b)) \Big|_{\sigma_k = \sigma_b} + \dots \end{aligned} \quad (\text{A4})$$

Inserting into Eqn. (A3) and cancelling a factor of $(\sigma_k - \sigma_b)$, we obtain,

$$-g^2 = \frac{-16\pi a \sqrt{\sigma_b}}{ia \frac{\partial}{\partial \sigma_k} (q_{2k}^*(\sigma_k)) \Big|_{\sigma_k = \sigma_b}} \quad (\text{A5})$$

Since $\partial q_{2k}^*/\partial \sigma_k = 1/4\sqrt{\sigma_k - 4m^2}$, we can write the residue as,

$$\begin{aligned} g &= 8\sqrt{\frac{\pi\sqrt{\sigma_b(\sigma_b - 4m^2)}}{i}} \\ &= 8\sqrt{\frac{\pi\sqrt{\sigma_b(-4/a^2)}}{i}} \\ &= 8\sqrt{\frac{2\pi\sqrt{\sigma_b}}{a}} \end{aligned} \quad (\text{A6})$$

Appendix B: Calculation of Pole Residue in Combined Bound State and Resonance Channel Case

Near the bound state, the pole on the real axis again takes the form,

$$\lim_{\sigma_k \rightarrow \sigma_b} \mathcal{M}_{2,RS+BS}(\sigma_k) = \frac{-g^2}{\sigma_k - \sigma_b} \quad (\text{B1})$$

Where g is the residue at the pole. Solving analytically for g , we find,

$$-g^2 = \lim_{\sigma_k \rightarrow \sigma_b} (\sigma_k - \sigma_b) \frac{\mathcal{K}_2(\sigma_k)}{1 - i\rho(\sigma_k)\mathcal{K}_2(\sigma_k)} \quad (\text{B2})$$

We can then expand the denominator as a Taylor series at $\sigma_k = \sigma_b$ as,

$$\begin{aligned} 1 - i\rho(\sigma_k)\mathcal{K}_2(\sigma_k) &= \overbrace{(1 - i\rho(\sigma_b)\mathcal{K}_2(\sigma_b))}^0 + (\sigma_k - \sigma_b) \frac{\partial}{\partial \sigma_k} \left(1 - i\rho(\sigma_k)\mathcal{K}_2(\sigma_k) \right) \Big|_{\sigma_k = \sigma_b} \\ &\quad + (\sigma_k - \sigma_b) \frac{\partial^2}{\partial \sigma_k^2} \left(1 - i\rho(\sigma_k)\mathcal{K}_2(\sigma_k) \right) \Big|_{\sigma_k = \sigma_b} + \dots \end{aligned} \quad (\text{B3})$$

Inserting into Eqn. (B2) and cancelling a factor of $(\sigma_k - \sigma)$, we obtain,

$$-g^2 = \frac{\mathcal{K}_2(\sigma_b)}{-i \frac{\partial}{\partial \sigma_k} \left(\rho(\sigma_k)\mathcal{K}_2(\sigma_k) \right) \Big|_{\sigma_k = \sigma_b}} \quad (\text{B4})$$

Taking,

$$\begin{aligned} \rho(\sigma_k) &= \frac{i\sqrt{4m^2 - \sigma_k}}{32\pi\sqrt{\sigma_k}} & \mathcal{K}_2(\sigma_k) &= \frac{g_1^2}{m_1^2 - \sigma_k} + \frac{g_2^2}{m_2^2 - \sigma_k} \\ &= \frac{i\sqrt{4m^2/\sigma_k - 1}}{32\pi} & &= \frac{g_1^2(m_2^2 - \sigma_k) + g_2^2(m_1^2 - \sigma_k)}{(m_1^2 - \sigma_k)(m_2^2 - \sigma_k)} \end{aligned}$$

Then the first order partial derivatives with respect to σ_k become,

$$\frac{\partial}{\partial \sigma_k} \rho(\sigma_k) = \frac{-im^2}{16\pi\sigma_k^{3/2}\sqrt{4m^2 - \sigma_k}} \quad \frac{\partial}{\partial \sigma_k} \mathcal{K}_2(\sigma_k) = \frac{g_1^2(m_2^2 - \sigma_k)^2 + g_2^2(m_1^2 - \sigma_k)^2}{(m_1^2 - \sigma_k)^2(m_2^2 - \sigma_k)^2}$$

Therefore the product rule gives,

$$\begin{aligned} \frac{\partial}{\partial \sigma_k} \left(\rho(\sigma_k)\mathcal{K}_2(\sigma_k) \right) &= \frac{i}{16\pi\sqrt{\sigma_k}(m_1^2 - \sigma_k)(m_2^2 - \sigma_k)} \left\{ \frac{1}{2}\sqrt{4m^2 - \sigma_k} \left(\frac{g_1^2(m_2^2 - \sigma_k)^2 + g_2^2(m_1^2 - \sigma_k)^2}{(m_1^2 - \sigma_k)(m_2^2 - \sigma_k)} \right) \right. \\ &\quad \left. - \frac{m^2}{\sigma_k\sqrt{4m^2 - \sigma_k}} (g_1^2(m_2^2 - \sigma_k) + g_2^2(m_1^2 - \sigma_k)) \right\} \end{aligned} \quad (\text{B5})$$

Therefore, after minor algebraic rearrangements, the full analytic expression for the residue at the pole becomes,

$$\begin{aligned} g^2 &= -16\pi\sqrt{\sigma_b} \frac{\sigma_b\sqrt{4m^2 - \sigma_b}}{g_1^2(m_2^2 - \sigma_b) + g_2^2(m_1^2 - \sigma_b)} \left\{ g_1^2(m_2^2 - \sigma_b) \left(\frac{\sigma_b(4m^2 - \sigma_b)}{2(m_1^2 - \sigma_b)} - m^2 \right) \right. \\ &\quad \left. + g_2^2(m_1^2 - \sigma_b) \left(\frac{\sigma_b(4m^2 - \sigma_b)}{2(m_2^2 - \sigma_b)} - m^2 \right) \right\}^{-1} \end{aligned} \quad (\text{B6})$$

Appendix C: Derivation of Intensity Observable

For the three-body case, the probability density for scattering is proportional to,

$$\text{Probability} \propto \int_0^{(\sqrt{s}-m)^2} \frac{d\sigma_p}{\pi} \int_0^{(\sqrt{s}-m)^2} \frac{d\sigma_k}{\pi} \rho(\sigma_p) \tau(\sigma_p, s) \rho(\sigma_k) \tau(\sigma_k, s) \left| \mathcal{M}_3(\sigma_p, \sigma_k) \right|^2 \quad (\text{C1})$$

Where,

$$\rho(\sigma_k) = \frac{q_k^*}{16\pi\sqrt{\sigma_k}} \quad \tau(s, \sigma_k) = \frac{k}{8\pi\sqrt{s}}$$

Since, in this regime, $\mathcal{M}_3(\sigma_p, \sigma_k) = \mathcal{M}_2(\sigma_p) d_S(\sigma_p, \sigma_k) \mathcal{M}_2(\sigma_k)$, we can denote Eqn. (C1) as $I(s)$ and expand as,

$$I(s) = \int_0^{(\sqrt{s}-m)^2} \frac{d\sigma_p}{\pi} \int_0^{(\sqrt{s}-m)^2} \frac{d\sigma_k}{\pi} \rho(\sigma_p) \tau(\sigma_p, s) \rho(\sigma_k) \tau(\sigma_k, s) \left| \mathcal{M}_2(\sigma_p) \mathcal{M}_2(\sigma_k) d_S(\sigma_p, \sigma_k) \right|^2 \quad (\text{C2})$$

From the two-body unitarity condition, we have $\text{Im} \mathcal{M}_2(\sigma_k) = \rho(\sigma_k) \left| \mathcal{M}_2(\sigma_k) \right|^2$. For the two-body amplitudes containing a bound-state pole (e.g. $\mathcal{M}_{2,BS}$ and $\mathcal{M}_{2,RS+BS}$), we can expand the imaginary part of the two-body scattering amplitude over the region of interest as,

$$\text{Im} \mathcal{M}_2(\sigma_k) = g^2 \pi \delta(\sigma - \sigma_b) + \rho(\sigma_k) \left| \mathcal{M}_2(\sigma_k) \right|^2 \Theta(\sigma - 4m^2) \quad (\text{C3})$$

Where the first term is the contribution from the pole in terms of the residue, and the second term contains a Heaviside function to include contributions from the physical region where $\sigma_k > 4m^2$. Inserting this expansion into Eqn. (C2),

$$\begin{aligned} I(s) &= \tau^2(\sigma_b, s) g^4 \left| d_S(\sigma_b, \sigma_b) \right|^2 \\ &+ 2 \int_{4m^2}^{(\sqrt{s}-m)^2} \frac{d\sigma_k}{\pi} \tau(\sigma_k, s) \tau(\sigma_b, s) g^2 \rho(\sigma_k) \left| d_S(\sigma_b, \sigma_k) \mathcal{M}_2(\sigma_k) \right|^2 \\ &+ \int_{4m^2}^{(\sqrt{s}-m)^2} \frac{d\sigma_k}{\pi} \int_{4m^2}^{(\sqrt{s}-m)^2} \frac{d\sigma_p}{\pi} \rho(\sigma_p) \tau(\sigma_p, s) \rho(\sigma_k) \tau(\sigma_k, s) \left| \mathcal{M}_2(\sigma_p) \mathcal{M}_2(\sigma_k) d_S(\sigma_p, \sigma_k) \right|^2 \end{aligned} \quad (\text{C4})$$

Recognizing $\tau(\sigma_b, s) = \rho_{\varphi b}(s)$, $\mathcal{M}_{\varphi b}(s) = g^2 d_S(\sigma_b, \sigma_b)$, and $\mathcal{M}_{\varphi b \rightarrow 3\varphi}(\sigma_k, s) = g \mathcal{M}_2(\sigma_k) d_S(\sigma_b, \sigma_k)$, we can express Eqn. (C4) as,

$$\begin{aligned} I(s) &= \left| \rho_{\varphi b}(s) \mathcal{M}_{\varphi b}(s) \right|^2 + 2 \int_{4m^2}^{(\sqrt{s}-m)^2} \frac{d\sigma_k}{\pi} \rho(\sigma_k) \tau(s, \sigma_k) \rho_{\varphi b}(s) \left| \mathcal{M}_{\varphi b \rightarrow 3\varphi}(\sigma_k, s) \right|^2 \\ &+ \int_{4m^2}^{(\sqrt{s}-m)^2} \frac{d\sigma_k}{\pi} \int_{4m^2}^{(\sqrt{s}-m)^2} \frac{d\sigma_p}{\pi} \rho(\sigma_p) \rho(\sigma_k) \tau(\sigma_p, s) \tau(\sigma_k, s) \left| \mathcal{M}_3(\sigma_p, s, \sigma_k) \right|^2 \end{aligned} \quad (\text{C5})$$

Appendix D: Bound State Only Additional Figures

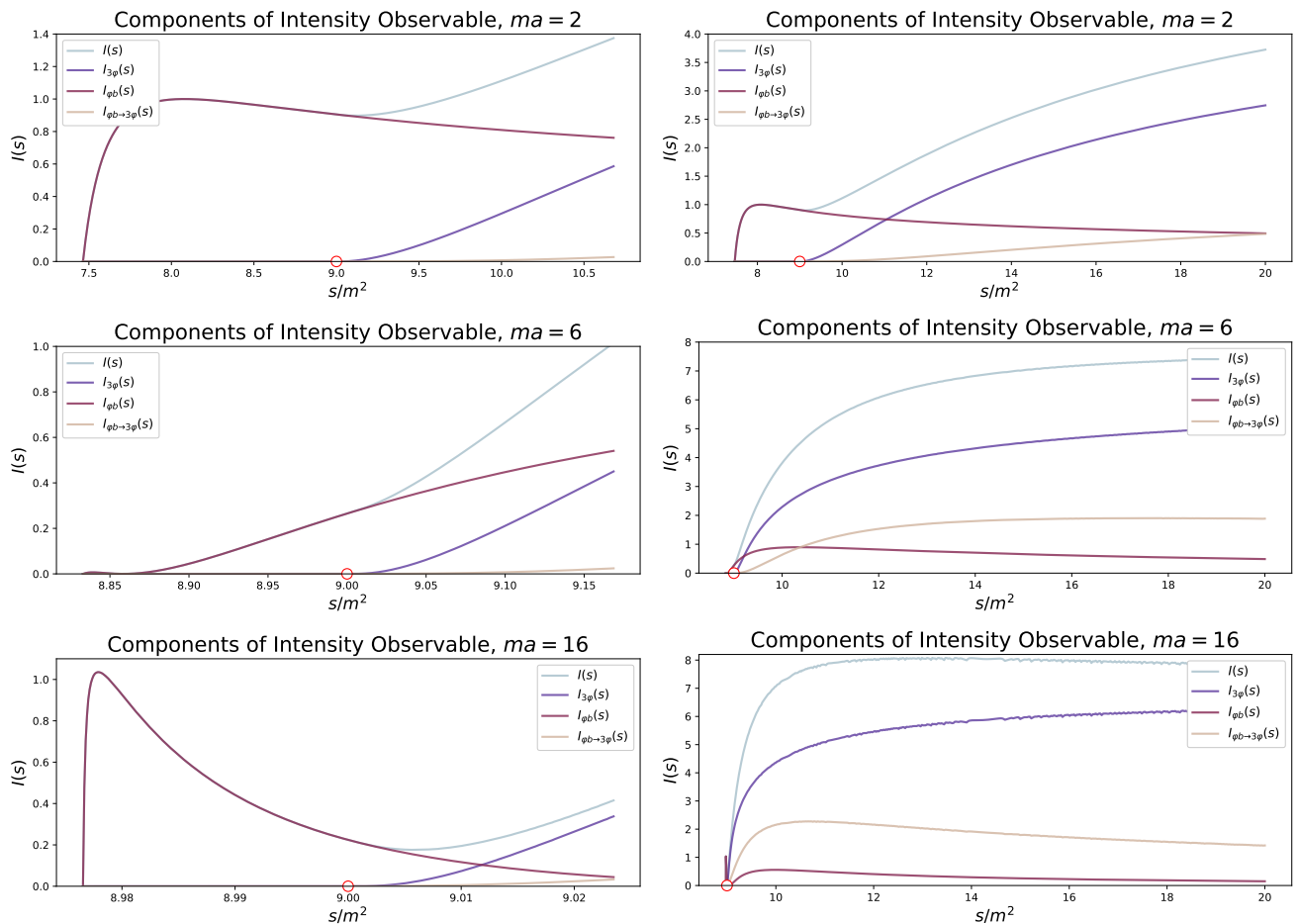


FIG. 8: Plots of $I(s)$ with varying underlying two-body bound state scattering lengths in the two energetic ranges of interest, as a function of s/m^2 . Each case is broken out by individual component contributions to the total intensity distribution. The red circles indicate the location of the three-body energetic threshold.

Above we have the full results for each of the scattering lengths of interest. The panels on the left are plotted over the symmetric energy range about the three particle energetic threshold given by $\sigma_b < s < 2(3m)^2 - \sigma_b$. The panels on the right extend the upper energy range to a fixed value of $s = 20m^2$. Going from top to bottom, we show results for each scattering length $ma = \{2, 6, 16\}$.

With increasing scattering length, the binding energy of the bound state decreases, and therefore we see the contributions from the $I_{\varphi b}$ components weaken. In particular, we note the phase-space available for the bound state in the case of $ma = 16$ is insignificant enough that the $I_{3\varphi}$ and $I_{\varphi b \to 3\varphi}$ components dominate the intensity distribution above the three-particle threshold.

-
- [1] M. T. Hansen, R. A. Briceño, R. G. Edwards, C. E. Thomas, and D. J. Wilson (2020), 2009.04931.
 - [2] A. W. Jackura, R. A. Briceño, S. M. Dawid, M. H. E. Islam, and C. McCarty, Phys. Rev. D **104** (2021), 2010.09820.
 - [3] A. Jackura, C. Fernández-Ramírez, V. Mathieu, M. Mikhasenko, J. Nys, A. Pilloni, K. Saldaña, N. Sherrill, and A. Szczepaniak (JPAC), Eur. Phys. J. C **79**, 56 (2019), 1809.10523.
 - [4] M. T. Hansen and S. R. Sharpe, Phys. Rev. **D92**, 114509 (2015), 1504.04248.